

Structural Characterization and Cytotoxic Properties of a 4-*O*-Methylglucuronoxylan from *Castanea sativa*

Charlotte Moine,[†] Pierre Krausz,[†] Vincent Chaleix,[†] Odile Sainte-Catherine,[‡] Michel Kraemer,[‡] and Vincent Gloaguen^{*†}

Laboratoire de Chimie des Substances Naturelles, EA 1069, Faculté des Sciences et Techniques, Université de Limoges, F-87060, France, and Laboratoire d'Oncologie Cellulaire et Moléculaire, EA 3410, Université Paris 13, F-93017, France

Received July 20, 2006

A glucuronoxylan was purified from a delignified holocellulose alkaline extract of *Castanea sativa* (Spanish chestnut) and its structure analyzed by means of FT-IR, GC of the *per*-trimethylsilylated methylglycoside derivatives, and ¹H and ¹³C NMR spectroscopy. The results supported a structure based on a linear polymer of xylopyranose units linked with $\beta(1\rightarrow4)$ bonds in which, on average, one out of every six units is substituted at C-2 by a 4-*O*-methylglucuronic acid unit; this structure is typical of a hardwood acidic 4-*O*-methylglucuronoxylan (MGX) with an estimated degree of polymerization of 200. The MGX from *C. sativa* inhibited the proliferation of A431 human epidermoid carcinoma cells with an IC₅₀ value of 50 μ M. In addition, this xylan inhibited A431 cell migration and invasion. Preliminary experiments showing that secretion of metalloproteinases MMP2 and MMP9 by A431 tumor cells was inhibited by the purified *C. sativa* MGX strongly suggest that this mechanism of action may play a role in its antimigration and anti-invasive properties.

Xylans are the most common hemicelluloses and account for the major noncellulosic cell wall polysaccharide fraction of angiosperms (e.g., trees, grasses, and cereals), where they present many different compositions and structures.^{1,2} Few of these are actually used in industrial processes.³ In terrestrial plants, xylans display a variety of side chains attached to a linear $\beta(1\rightarrow4)$ -D-xylopyranose backbone, mainly single α -L-arabinofuranosyl and α -D-glucopyranosyl uronic acid (or its 4-*O*-methyl ether) units. In addition, L-rhamnose, D-xylose, D-galactose, D-glucose, and a variety of di- and trimeric side chains, as well as acetyl groups and phenolic acids, such as ferulic and coumaric acids, have been identified in various fractions that form a distinct family called heteroxylans (HX). A number of families of green and red algae are also able to synthesize xylans that contribute to the structure of their cell walls.⁴

Xylans are mainly located in the wood of dicotyledons and, with the exception of Poaceae, in monocotyledons in which glucuronoxylan (GX) and arabinoglucuronoxylan (AGX) represent between 25% and 35% of dry weight. Wood and wood byproducts, such as sawdust, are also rich in xylans. More precisely, 4-*O*-methyl- α -D-glucuronopyranosyl uronic acid xylan (MGX) is the major hemicellulose component of the cell wall of hardwood trees, where it can represent up to 20% (weight ratio) of NaClO₂-delignified wood.^{1,2} The most representative structure of this polysaccharide is a linear chain of $\beta(1\rightarrow4)$ Xyl_{*n*} units of which a few unevenly distributed residues are substituted at C-2 by 4-*O*-methylglucuronic acid.⁵ The Xyl_{*p*}/MeGlcA ratios range from 4:1 to 16:1 (10:1 on average).¹ The molecular mass of MGX varies between 5000 and 30 000 Da, with degrees of polymerization (DP) from 35 to 230.¹ These two last structural parameters depend, on one hand, on the extraction procedures and, on the other hand, on the botanical origin of the wood. Finally, the C-2 and/or the C-3 of Xyl_{*p*} can be acetylated.⁶ This explains the structural diversity of 4-*O*-methylglucuronoxylans.

Plant cell walls are also known to be potential sources of pharmacologically active polysaccharides,^{7–11} which, within the herbal medicine context, have long been thought as potential anti-inflammatory agents as well as wound-healing promoters.^{10,11} Carbohydrate-based therapeutics promises a new class of com-

pounds for controlling various disorders such as cancer, viral infections, and immune dysfunctions.^{10,11} Most information regarding the biological properties of pectic polysaccharides, $\beta(1\rightarrow3)$ -glucans, glucomannans, or arabinogalactans,⁹ is available in the literature,¹² but few studies have been published on the potential antitumor properties of MGX. The MGX from Japanese beechwood has been reported to inhibit the growth rate of sarcoma-180 and other tumors, probably due to the indirect stimulation of the nonspecific immunological host defense;^{13,14} however, no conclusions were made about the structural and molecular features that determine the biological activity of this xylan.

Many primary tumors are able to spread by invasion and metastasis via tumoral angiogenesis¹⁵ and tumoral lymphangiogenesis.¹⁶ In order to metastasize from the primary tumor, the tumor cells have to migrate through the extracellular matrix and the basement membrane before entering new vessels. The migration of tumor cells is related to the degradation of the individual components of the extracellular matrix via the secretion and activation of proteolytic enzymes.

The aim of the present study was, first of all, to establish an extraction procedure and a subsequent purification protocol and to study the structure of the MGX from *Castanea sativa* Mill. (Fagaceae) (Spanish chestnut; sweet chestnut), a common tree of the Limousin region (France). Then the *in vitro* proliferation-inhibiting effects of the MGX on five human tumor cell lines was investigated. In addition, the effects of purified *C. sativa* MGX on the A431 vulvar epidermal carcinoma cell line, more precisely on cell migration and invasion, as well as the cell cycle and apoptosis were examined.

Results and Discussion

The experimental procedures for the extraction of biomolecules from plant material have to be able to sufficiently extract a major class of molecules under consideration and must also limit degradation during the extraction process. The presence of close interactions between xylans and the lignin within the cell wall of wood reduces their extractability. In the case of hardwood derivatives prepared as sawdust, a preliminary delignification is considered a first step that aids extraction of the cell wall xylan.⁴ Moreover, a dilute KOH pretreatment, by inducing the swelling of cell wall fibers, can also improve the extractability of cell wall polysaccharides. In the case of *C. sativa*, this last step had no positive impact and was omitted in the present study.

* Corresponding author. E-mail: vincent.gloaguen@unilim.fr. Tel: (33)-555457481. Fax: (33)555457202.

[†] Université de Limoges.

[‡] Université de Paris 13.

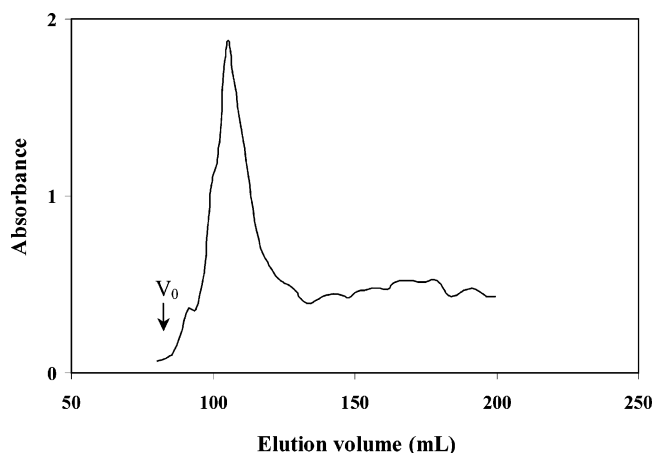


Figure 1. Size exclusion chromatography of *C. sativa* MGX using a Sepharose CL-4B column. Sugars were detected according to the phenol sulfuric acid method, and absorbances were measured at 492 nm. V_0 : Void volume.

From a quantitative point of view, the KOH extract isolated from *C. sativa* represented up to 19% of the initial sawdust dry mass. This value is in good agreement with data published by Alèn,¹⁷ which indicated that GX of wood represents from 20% to 30% of the dry material depending of the origin of the wood. With 76.3% of Xyl and 14.6% of 4-*O*-MeGlcA (molar ratio), the KOH extract represented the typical characteristics of a 4-*O*-methylglucuronoxylan (MGX). Traces of Ara (0.8%), Rha (1.8%), Man (0.8%), Gal (2.0%), Glc (1.0%), GalA (2.1%), and GlcA (0.6%) were also detected and could be considered as contaminants. The FT-IR spectrum of the native molecule showed a main band maximum at 1044 cm^{-1} , which could be attributed to ring vibrations and stretching vibrations of (C–OH) side groups.^{18,19} An absorbance at 1165 cm^{-1} represented the glycosidic bond $\nu(\text{C–O–C})$ contribution.²⁰ A small sharp band at 897 cm^{-1} was characteristic of β -glycosidic linkages between the sugar units.^{21,22} Absorbances at 1329 and 1416 cm^{-1} were associated with C–H bending and wagging and O–H bending.^{23,24} An intense residual water band at 1644 cm^{-1} and a band of uronic acid carboxylate at 1605 cm^{-1} were also observed. The mass polydispersity of MGX was then studied using size exclusion chromatography on a Sepharose CL-4B column. In the chromatographic conditions used for the filtration, *C. sativa* MGX was eluted as a narrow peak characteristic of a polymer with low polydispersity (Figure 1). Moreover, based on colorimetric estimation, the ratio of the reducing sugar to the total carbohydrate suggests that *C. sativa* MGX has an average DP of 200, or a mass close to 30 000 Da.

From a structural point of view, NMR spectroscopic analysis can provide all the information required to establish the structure of a MGX. It is thus possible to assay and identify each monosaccharide unit, to characterize branching points and their anomeric configuration, and to determine the sequence of monomers. ^1H and ^{13}C NMR spectra are given in Figures 2 and 3, respectively, for the *C. sativa* MGX. The complete assignment of the proton and carbon spectra (chemical shifts reported in Table 1) was achieved by performing 2D COSY and 2D HMQC experiments.

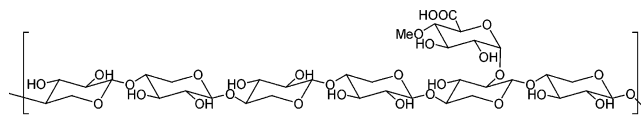
Examination of data relative to ^1H NMR analysis revealed three important groups of protons: major signals corresponding to the nonsubstituted backbone D-xylose units and two groups of minor signals, with the first corresponding to the 4-*O*-Me-D-GlcA residues and the second assigned to D-Xyl units substituted with 4-*O*-Me-D-GlcA. From the fact that the coupling constants for the anomeric protons of xylose units, substituted (at 4.5 ppm) or nonsubstituted (at 4.6 ppm), were larger than 7 Hz, the xylose residues were shown to be linked via β -glycosidic bonds, while the anomeric proton of 4-*O*-Me- α -D-GlcA exhibited a doublet with a coupling constant

less than 2 Hz, corresponding to an α -configuration. In addition, the presence of the methyl group of MeGlcA was confirmed by a corresponding sharp singlet at 3.46 ppm. The linkage via (1 \rightarrow 2) glycosidic bonds between Xyl and 4-*O*-MeGlcA was confirmed by the deshielding of the H-2 signal of the substituted Xyl (3.44 ppm), by comparison with the nonsubstituted one (3.29 ppm).

By using a HMQC 2D experiment, the ^{13}C NMR spectrum was completely assigned for the *C. sativa* MGX from the proton spectrum (chemical shifts reported in Table 1). The ^{13}C NMR spectrum contained five major signals corresponding to that of a (1 \rightarrow 4)-linked- β -xylan.⁶ The signal at 102.09 ppm corresponded to the anomeric region in a β -configuration, as confirmed by the ^1H NMR spectrum, while the signals at 76.76, 74.07, and 73.11 ppm corresponded to C-4, C-3, and C-2, respectively, and the 63.38 ppm signal arose from C-5. Minor differences were observed for ^{13}C NMR chemical shifts of substituted xylose units, especially at the C-2-substituted position. Concerning the glucuronic unit, the signal of the methoxylated C4 appeared at 82.89 ppm and the carbon signal for the methoxyl group was found at 60.29 ppm. Last, the carboxyl was observed at 177.21 ppm. These data are in agreement with those reported in the literature for related 4-*O*-methylglucuronoxylans.²⁵

The relative amounts of Xyl and 4-*O*-Me- α -D-GlcA were determined by integration of the corresponding anomeric protons, and the ratio Xyl/4-*O*-MeGlcA was subsequently calculated. Integration results gave an approximate value of 5.9:1, in agreement with GC analysis. This value obtained for this xylan from *C. sativa* wood examined here is typical of hardwood xylans.

On the basis of the experimental data obtained from GC and NMR analyses, a theoretical structural model can be proposed for the MGX repeating unit of *C. sativa* as follows:



This polymer is formed by a linear backbone of six (β -1 \rightarrow 4)-linked xylopyranosyl residues. At least one of the xylose residues is monosubstituted at C-2 by a 4-*O*-methylglucuronic acid, giving for *C. sativa* a typical ratio of 4-*O*-methyl glucuronic acid to Xyl of 1 to 6. Owing to its characteristic large content of carboxyl functions, the MGX from *C. sativa* can be classified as an acidic xylan.

To investigate the effects of MGX on the cell proliferation, tumor cells were treated with increasing doses of xylan ranging from 0.8 to 50 μM (Figure 4). The *C. sativa* MGX inhibited tumor cell proliferation, and the concentration inducing 50% of maximal inhibition (IC_{50}) was determined. The IC_{50} value was 50 μM for A431 cells. For the other cell lines, the IC_{50} could not be evaluated and the maximum inhibitions observed at 50 μM were 45%, 27%, 26%, and 41% for DU145, HT1080, MDA-MB-231, and HuH7 cell lines, respectively. As the A431 cell line was the most sensitive to cell proliferation inhibition by this MGX, we then focused our attention specifically on these cells. A431 human squamous cell carcinoma cells represent a good model of an aggressive, highly angiogenic, and invasive tumor.^{26,28} A431 cells display an increase of epidermal growth factor receptors (EGFR) and produce large amounts of vascular endothelial growth factor (VEGF),²⁹ promoting neovascularization.³⁰ Increased EGFR expression renders A 431 cells less dependent upon an exogenous source of epidermal growth factor (EGF) and enhances the EGF-induced mitogenic responses of squamous cell carcinoma cell lines compared with human epidermal keratinocytes, contributing to the invasiveness of malignant cells.³¹

In the presence of a chemotactic stimulus (FCS) in the lower part of the Boyden migration chamber, the A431 cells migrated through the pores to the lower surface of the membrane (Figure 5). The

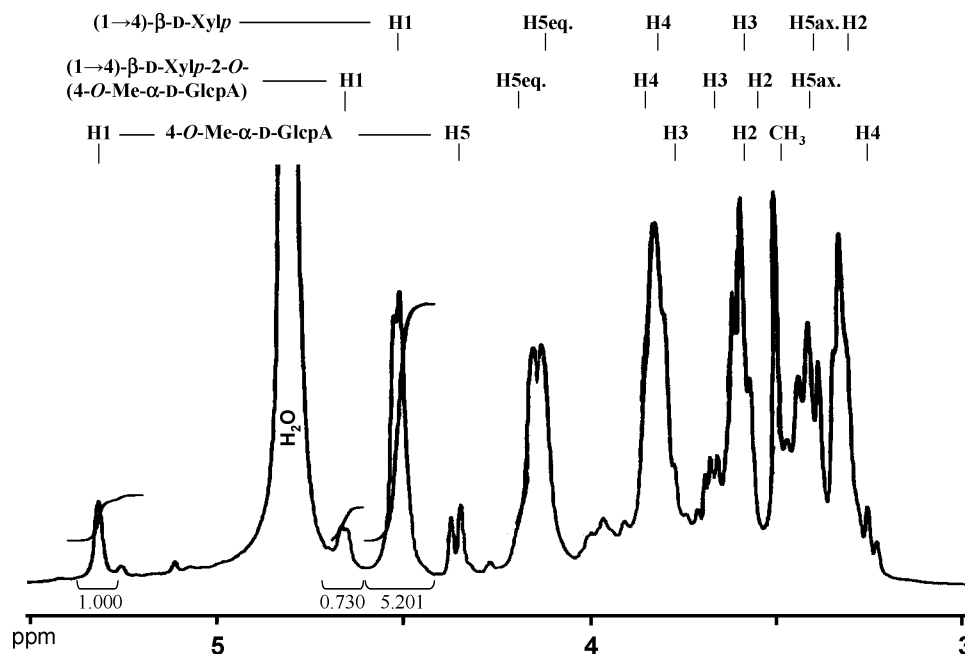


Figure 2. ^1H NMR spectrum of *C. sativa* MGX. Solvent is D_2O at 300 K; numerical values are in δ (ppm).

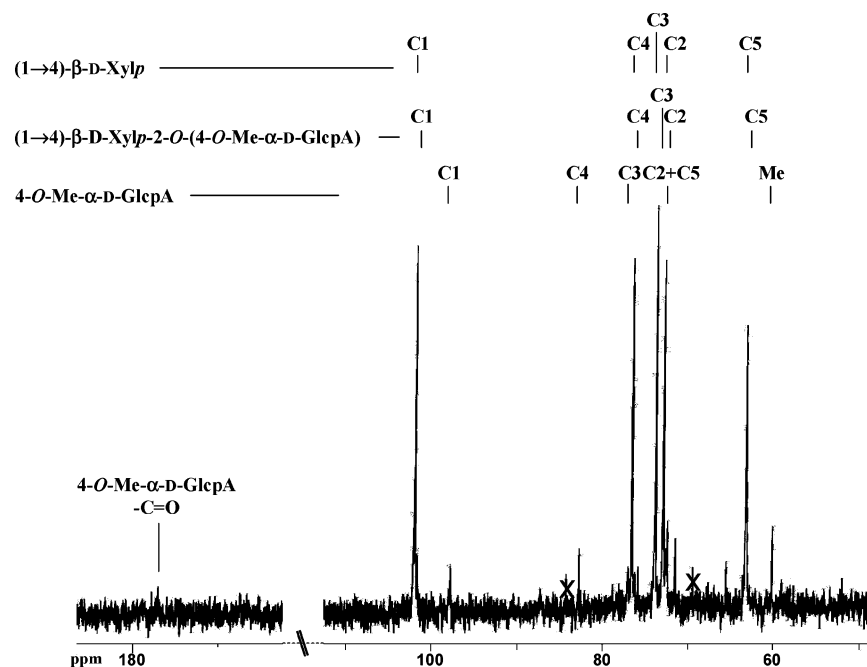


Figure 3. ^{13}C NMR spectrum of *C. sativa* MGX. Solvent is D_2O at 300 K; numerical values are in δ (ppm).

Table 1. ^1H and ^{13}C NMR Chemical Shift (ppm) Assignments for Residues of *Castanea sativa* Xylan (MGX), $^3J_{\text{H,H}}$ (Hz)

position	(1→4)-β-D-Xylp		(1→4)-β-D-Xylp-2-O-(4-O-Me-α-D-GlcpA)		4-O-Me-α-D-GlcpA	
	^1H	^{13}C	^1H	^{13}C	^1H	^{13}C
	δ (ppm) (J Hz)	δ (ppm)	δ (ppm) (J Hz)	δ (ppm)	δ (ppm) (J Hz)	δ (ppm)
1	4.48 d (7.5)	102.09	4.63 d (7.2)	101.79	5.29 d (2.0)	97.94
2	3.29 t (8.2)	73.11	3.44 m	76.03	3.60 m	72.64 ^b
3	3.55 t (9.0)	74.07	3.62 m	71.67 ^b	3.76 m	77.22
4	3.79 m	76.76	3.81 m	74.21	3.22 t (9.7)	82.89
5 _{ax}	4.10 dd (4.5; 11.5)	63.38	4.15 m	65.64	4.33 d (10.1)	72.76 ^b
5 _{eq}	3.38 t (11.0)		3.42 m			
6						177.21
O-CH ₃					3.46 s	60.29

^a Ax = axial, eq = equatorial. ^b Assignments may be interchanged.

MGX from *C. sativa* significantly reduced cell migration. Compared with untreated control cells, the migration of A431 was significantly decreased by 68% ($p < 0.05$) and 99% ($p < 0.05$) in the presence

of 5 and 50 μM MGX, respectively. A Matrigel invasion assay was performed to study the effect of MGX (5 and 50 μM) on the invasive ability of A 431 cells. MGX at 5 μM did not reduce the

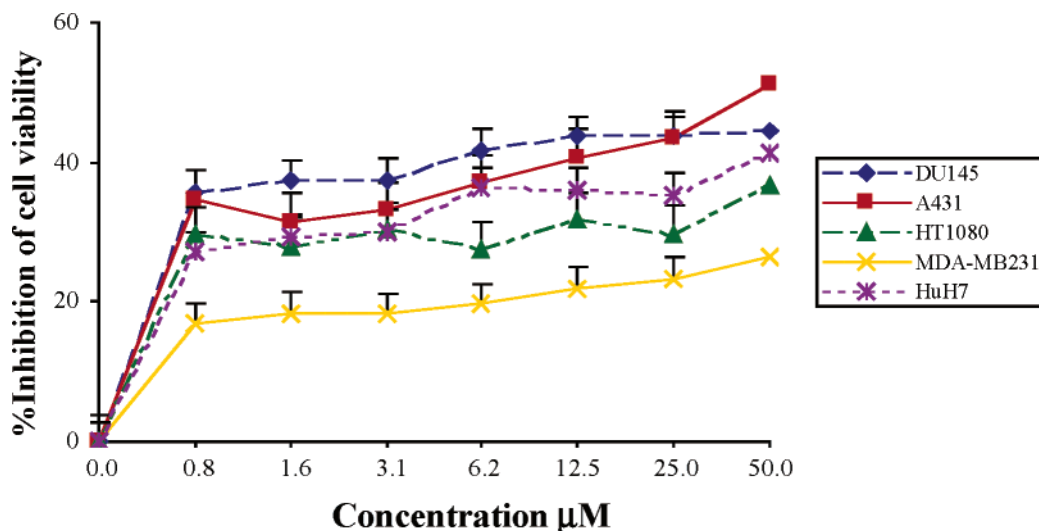


Figure 4. Dose-dependent effects of *C. sativa* MGX on DU145, A431, HT1080, MDA-MB-231, and HuH7 cell viability. DU145, A431, HT1080, and MDA-MB-231 cells were treated with increasing concentrations (0.8 to 50 μM) of this xylan for 72 h, and HuH7 cells were treated in a similar manner for 144 h. Results are mean \pm SEM of three independent experiments.

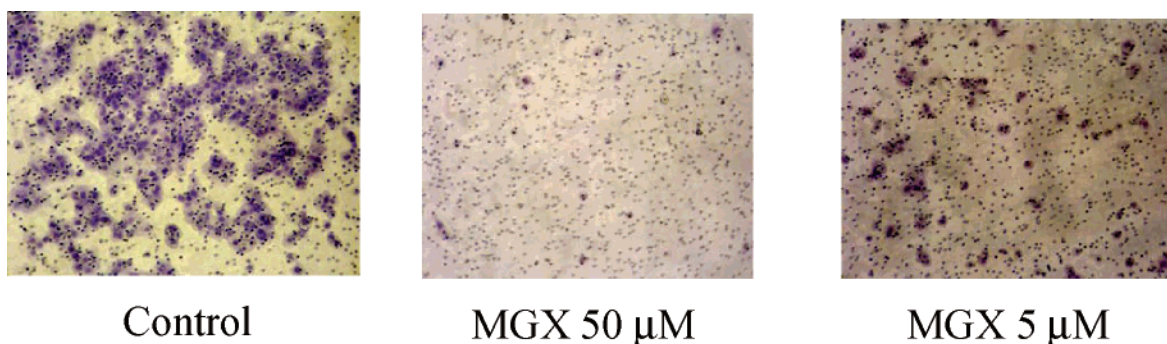


Figure 5. Effects of *C. sativa* MGX on the migration of A431 cells seeded on a fibronectin matrix in the upper chamber, with FCS 10% added to the lower chamber. Fewer cells migrated to the lower chamber in the presence of this xylan. The migration of A431 cells was inhibited by 68% and 99%, respectively, by MGX at 5 and 50 μM . Original magnification $\times 200$.

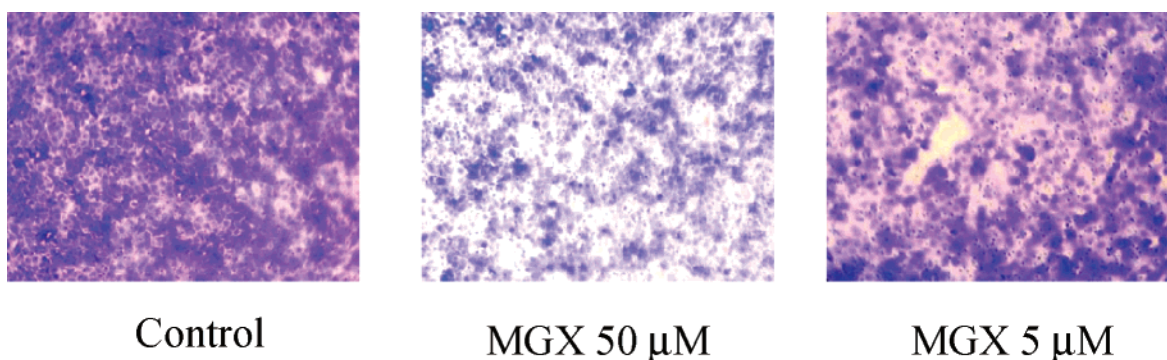


Figure 6. Effects of *C. sativa* MGX on the invasion of A431 cells seeded on a matrigel basement membrane matrix in the upper chamber, with FCS 10% added to the lower chamber. Fewer cells migrated to the lower chamber in the presence of MGX. The invasion of A431 cells was inhibited by 55% with MGX at 50 μM . No effect of MGX at 5 μM on cell invasion was demonstrated. Original magnification $\times 200$.

invasion of tumor cells, while at 50 μM (corresponding to the IC_{50}) this xylan reduced the invasion of A431 cells by 55% as compared with untreated control cells (Figure 6). Cell migration that takes place during angiogenesis requires the degradation of the extracellular matrix by proteases as matrix metalloproteases (MMP).³² Since MGX inhibited migration and the invasion of A431 cells, it was then examined by zymography to determine if this compound could affect the secretion of MMP9 and MMP2 gelatinases by A431 cells. As shown in the zymogram of Figure 7, untreated A431 cells secreted ProMMP9, ProMMP2, and active forms of MMP9. Exposure of these cells to 12.5 μM MGX resulted in a significant

time-dependent inhibition of ProMMP9 and ProMMP2. Analysis by quantitative zymography indicated that the amount of ProMMP secreted in the medium and normalized to cell number after 48 and 72 h of treatment decreased by 17% and 56% for ProMMP2 and by 50% (for both treatment times, respectively) for ProMMP9. The expression of MMP9 was totally abolished in 24 h treated cells as compared to control cells. The antimigration and antiproliferative effects of MGX can therefore be explained, at least in part, by a decrease of the expression of MMP9 and MMP2.

To study the cellular mechanism underlying *C. sativa* MGX-induced A431 cell proliferation inhibition, we then performed cell

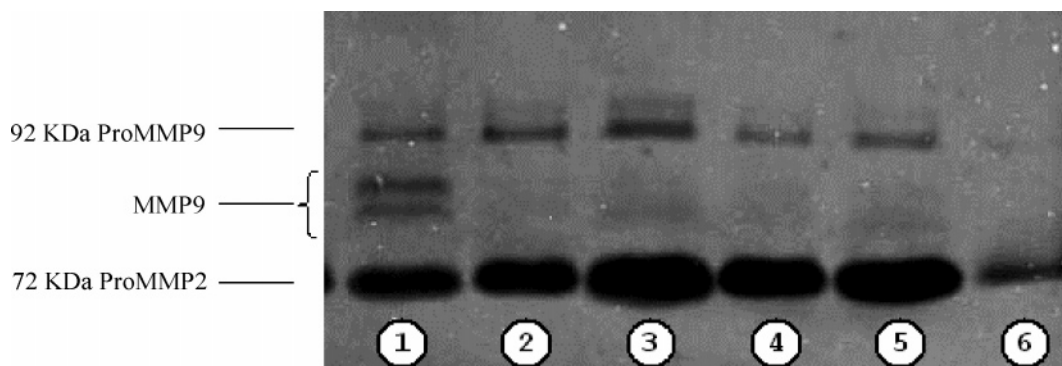


Figure 7. Effects of *C. sativa* MGX on ProMMP9, MMP9, and ProMMP2 secretion by A431 cells. Gelatin zymography of serum-free conditioned media from A431 cell cultures. Conditioned media from untreated cell cultures (lanes 1, 3, and 5) or cell cultures treated with 12.5 μ M MGX (lanes 2, 4, and 6) were collected after 24, 48, or 72 h of incubation, normalized to cell number, and subjected to gelatin zymography. Lane 1, nontreated cells for 24 h; lane 2, treated cells for 24 h; lane 3, nontreated cells for 48 h; lane 4, treated cells for 48 h; lane 5, nontreated cells for 72 h; lane 6, treated cells for 72 h.

cycle analysis and apoptosis detection. The MGX at different concentrations (50, 75, and 100 μ M) did not exhibit any inhibitory effect on the different phases of the cell cycle as compared with untreated control cells. Incubation of A431 cells for 72 h with different concentrations of the MGX (50, 75, and 100 μ M) induced apoptosis in a dose-dependent manner (respectively 12%, 19%, and 21%), as compared to untreated cells (5% of apoptotic cells). After 3 days of treatment, other features of apoptosis on A431-treated cells were observed, such as peripheral cytoplasmic budding and the appearance of apoptotic bodies. Inhibition of A431 cell proliferation would then be most likely related to an induction of apoptosis rather than to cell cycle inhibition.

Plant cell walls are known as potential sources of pharmacologically active polysaccharides. Even though there is an abundant literature regarding the biological properties of plant xylans, few data have been published on the potential antitumor activity of 4-*O*-methylglucuronoxylans from wood. Hashi and Takeshita^{13,14} reported the inhibition of sarcoma-180 and other tumor systems by Japanese beechwood MGX. The authors explained this phenomenon by the indirect stimulation of the nonspecific immunological host defense. The present work demonstrates that MGX from *C. sativa* directly acts by inhibiting proliferation, invasion, and migration of highly invasive A431 tumor cells. One possible mechanism inducing tumor cell death is by induction of apoptosis. Taken together, our results suggest that this MGX could be very efficient in eradicating aggressive tumors.

Recently, Ebringerova and co-workers³³ used the comitogenic thymocyte test in order to check the properties of MGXs extracted from beechwood and three medicinal herbs, *Rudbeckia fulgida*, *Althaea officinalis*, and *Mahonia aquifolium*. These polymers exhibit different molecular weights (between 17 000 and 37 000 Da), compositions (ratio Xyl:MeGlcA between 6.4:1 and 8.4:1), and distributions (random or regular) of MeGlcA substituents. Since they reflect the fine structure of the macromolecular chains, these parameters may affect the intermolecular interactions between xylan molecules in solution creating networks or microgels, as well as interactions with the thymocyte cell coat.³³ Comparison of the biological responses of the tested acidic xylans did not reveal any unequivocal relation to either molecular weight, MeGlcA content, or distribution patterns. Experimental clues leading to an identification of the individual structural parameters having an influence on the immunological effects are yet to come.

For pectins¹² and β (1 \rightarrow 3) glucans,³⁴ many suggestions have been proposed to explain the biological properties of these polymers. They refer to the glycosidic linkages of the polymer backbone and/or its ramifications, the degree of branching, the molecular mass, polyanionic characteristics, and helical structure.⁸ It is now accepted that not only the primary structure but also the whole complex of

chemical and physicochemical properties and supramolecular structural features of these polymers may altogether contribute to the expression of their biological properties. To amplify this structure–function relationship, we have started a study on the three-dimensional structure, in which xylans appear as highly organized helical macromolecules.³⁵ Additional work should be done in order to identify the carbohydrate sequence(s) and/or the chemical group(s) responsible for these phenomena. To this end, it would be interesting to investigate the biological properties of oligo-MeGXs of known structure obtained by means of chemical degradation or enzymatic hydrolysis by endo- β (1 \rightarrow 4)-xylanase.

Further *in vivo* experiments in suitable animal models are required to determine whether the MGX from *C. sativa* is clinically relevant for the treatment of carcinomas.

Experimental Section

General Experimental Procedures. All extracts (see below) were evaporated at <40 $^{\circ}$ C under reduced pressure. The centrifugation conditions were 10 000 rpm for 15 min at 25 $^{\circ}$ C. Total carbohydrate was measured by the phenol sulfuric acid method.³⁶ Hexuronic acids were determined with the *meta*-hydroxy-diphenyl method.³⁷ The content of reducing sugars was estimated according to the method of Lever.³⁸ The FT-IR spectrum of native 4-*O*-methylglucuronoxylan (MGX) was recorded on a KBr pellet using a Perkin-Elmer FT-IR Spectrum 1000 spectrometer in the frequency range 400 to 4000 cm^{-1} . Separation of *per*-trimethyl-silylated methylglycosides was done with a Perichrom gas chromatograph fitted with a flame-ionization detector. A capillary column, CPSIL-5CB (Chrompack, 0.32 mm \times 50 m), was used with the following temperature program: 120 to 240 $^{\circ}$ C at 2 $^{\circ}$ C \cdot min $^{-1}$. Nitrogen was the carrier gas at 0.5 atm.

Plant Material. *Castanea sativa* Mill., identified by Dr. G. Saladin, a botanist at the University of Limoges, was collected in the Limousin region of France in October 2004. Voucher specimens were deposited in the Life Sciences Department of the University of Limoges under the references CsM1-2004 and CsM2-2004. Sawdust from these samples was prepared from a local sawmill. The taxonomist verified that sawdust was from *C. sativa*.

Isolation and Purification of the 4-*O*-Methylglucuronoxylan (MGX). Sawdust of *C. sativa* was dried for 48 h at 60 $^{\circ}$ C in a ventilated oven and ground to pass through a 500 μ m-size sieve. Forty-five grams of ground sawdust was then extracted in a Soxhlet extractor with 80% EtOH and freeze-dried before further purification. The dewaxed sawdust was then sequentially depectinized using 1% ammonium oxalate solution (1 h at 80 $^{\circ}$ C) and delignified by addition of an acidic sodium chlorite solution (0.47 g of sodium chlorite and 0.2 mL of glacial acetic acid per gram of sawdust) at 80 $^{\circ}$ C for 1 h. After filtration, the residue was washed with water and then air-dried at 60 $^{\circ}$ C for 16 h to give 36 g of holocellulose. Then, the MGX was extracted from 10 g of holocellulose for 24 h at room temperature with a 4.3 M KOH solution containing 3 mg of NaBH₄ per mL, with continuous agitation under nitrogen. The hemicellulose solution was neutralized by addition of

glacial acetic acid and dialyzed against water (Spectrapor MWCO 6–8000 Da). Hemicelluloses were precipitated by the addition of 3 volumes of ethanol to the aqueous solution, with the pellet recovered after centrifugation, solubilized in water, and then freeze-dried for storage. Compared to holocellulose, the approximate yield of the *C. sativa* MGX was 23.7%.

Monosaccharide Composition. Monosaccharide determination was carried out after methanolysis (MeOH/HCl 0.5 N, 24 h, 80 °C) by gas-liquid chromatography of *per*-trimethyl-silylated methylglycosides according to Kamerling and co-workers,³⁹ modified by Montreuil and co-workers.⁴⁰

Mass Polydispersity. The mass polydispersity of MGX was studied using size exclusion chromatography on a 70 × 3 cm Sepharose CL-4B column (Pharmacia, range of mass exclusion 30 000 to 5 000 000 Da as dextran equivalent) with water elution.

NMR Analysis. Samples were freeze-dried three times in D₂O and then dissolved in 600 μL of D₂O (99.97% purity, Euriso-top, Saclay, France). The chemical shifts (ppm) were calibrated relative to the signals from acetone used as an internal standard, at 2.22 and 31.5 ppm for the ¹H and ¹³C NMR spectra, respectively. The samples were analyzed at 300 K in 5 o.d. mm BMS-005-B Shigemi tubes on a Bruker DPX-400 spectrometer operating at 400.13 (¹H) and 100.62 MHz (¹³C). The ¹H NMR spectrum was acquired using a 5.7 kHz width with 32 K data points, and 2.831 s acquisition time, and 152 scans were accumulated (¹H 90° pulse = 5.2 μs). The ¹³C NMR spectrum was obtained with a 26.2 kHz spectral width, 32 K data points, 0.62 s acquisition time, and 15 154 scans. The pulse programs of the two-dimensional experiments were taken from the Bruker software library, and the parameters were as follows: for 2D ¹H–¹H correlated spectroscopy (COSY), relaxation delay *d*₁ = 2 s, 90° pulse = 5.20 μs for ¹H, 2 048 data points in *t*₂, spectral width 10.483 ppm in both dimensions, 512 experiments in *t*₁; for 2D ¹³C–¹H heteronuclear multiple quantum coherence (HMQC) experiment, relaxation delay *d*₁ = 2 s, evolution delay, *d* = 3.44 ms, 90° pulse = 7.20 μs for ¹H, 11 μs for ¹³C hard pulse, and 80 μs for ¹³C cpd sequence, 1024 points in *t*₂, spectral width 10 ppm in *F*₂ and 189 ppm in *F*₁ and 512 experiment in *t*₁.

Xylan Solubilization. According to the solubility of the MGX, the stock solution was prepared at 0.5 mM in water. Dilutions of the stock solution were conducted with Eagle's medium, and the highest concentration tested corresponded to 0.05 mM.

Cell Lines and Cell Culture. Cell lines were cultured in Dulbecco's modified Eagle's medium (DMEM) supplemented with 10% fetal calf serum (FCS), 2 mM L-glutamine, 1 mM sodium pyruvate, 50 U mL⁻¹ streptomycin (all obtained from Life Technologies Inc.), at 37 °C in a 5% CO₂ humidified atmosphere. Human A431 squamous cell carcinoma (vulvar epidermoid carcinoma), breast carcinoma (MDA-MB-231), prostate carcinoma (DU145), fibrosarcoma (HT1080), and hepatocarcinoma (HuH7) cells were obtained from the American Type Culture Collection.

Cell Viability Experiments. Cell viability was evaluated using the MTT microculture tetrazolium assay,^{41–43} based on the ability of mitochondrial enzymes to reduce 3-(4,5-dimethylthiazol-2-yl)-2,5-diphenyltetrazolium bromide (MTT) (Sigma, St. Louis, MO) into purple formazan crystals. Cells were seeded at a density of 2.5 × 10³, 5 × 10³, 10 × 10³, 20 × 10³, and 50 × 10³ cells/well for HT1080, A431, DU145, MDA-MB-231, and HuH7 cells, respectively. Cells were seeded in 96-well flat-bottom plates (Falcon, Strasbourg, France) and incubated in complete culture medium for 24 h. Then, the medium was removed and replaced by 2% FCS-medium containing increasing concentrations of xylan varying from 0.8 to 50 μM. After 72 h incubation for HT1080, A431, DU145, and MDA-MB-231 cells, or 144 h for HuH7 cells, the cells were washed with phosphate-buffered saline (PBS, Life Technologies) and incubated with 0.1 mL of MTT (2 mg/mL, Sigma-Aldrich) for an additional 4 h at 37 °C. The insoluble product was then dissolved by addition of 200 μL of DMSO (Sigma-Aldrich). The absorbance corresponding to the solubilized formazan pellet (which reflects the relative viable cell number) was measured at 570 nm using a Labsystems Multiskan MS microplate reader. Concentration–response curves were constructed, and IC₅₀ values (concentration of the compound inhibiting 50% of cell proliferation) were determined. All in vitro cell experiments (viability, migration, and invasion assays) were carried out at 37 °C in a 5% CO₂ incubator.

Cell Migration Assay. The influence of MGX on the migration of A431 cells was investigated as described previously⁴² using Boyden invasion chambers with 8 μm pore size filters coated with 100 μL of

fibronectin (100 μg/mL, Santa Cruz Biotechnology, Santa Cruz, CA) and were allowed to stand overnight at 4 °C. Then, 3 × 10⁴ A431 untreated or 24 h MGX (at 50 or 5 μM)-pretreated A431 cells were added to each insert (upper chamber). A strong chemoattractant (10% FCS) for A431 cells was added to the lower chamber. After 24 h incubation at 37 °C in a 5% CO₂ incubator, nonmigrated cells were removed by scraping and migrated cells were fixed in methanol and stained with hematoxylin. Cells migrating on the lower surface of the filter were counted in 10 fields using a Zeiss microscope. Results were expressed as a percentage, relative to controls normalized to 100%. Experiments were performed in triplicate.

Cell Invasion Assay. Cell invasion experiments were performed with Boyden chambers as described above. The inserts were coated with Matrigel membrane matrix (Falcon, Becton Dickinson Labware, Bedford, MA). The A431 cells (5 × 10⁴) were seeded in the upper well of the Boyden chamber, and 10% FCS was added to the lower chamber.

Before seeding in the upper chamber, the cells were pretreated with MGX at 50 or 5 μM for 24 h. After 24 h at 37 °C in a 5% CO₂ incubator, noninvaded cells in the upper chamber were wiped with a cotton swab and the filters were fixed, stained, and counted. Results were expressed as a percentage, relative to controls normalized to 100%. Experiments were performed in triplicate.

Zymography. A431 cells were seeded at a density of 50 × 10⁴/well into six-well tissue culture plates in DMEM–10% FCS. Cells were allowed to adhere for 24 h and then incubated with 12.5 μM MGX. Conditioned media were collected 24, 48, or 72 h after treatment with MGX, normalized to cell number, mixed with nonreducing Laemmli sample buffer, and subjected to 10% SDS-PAGE containing 0.1% (w/v) gelatin. The gel was washed three times at room temperature in a solution containing 2.5% (v/v) Triton X-100 in H₂O and incubated at 37 °C for 24 h in 50 mM Tris/HCl, pH 7.4, 0.2 M NaCl, 5 mM CaCl₂, and 0.05% Brij 35. The gel was stained for 60 min with 0.5% (w/v) R-250 Coomassie blue in 30% methanol (v/v)/10% acetic acid (v/v). ProMMP9, MMP9, and ProMMP2 detection proceeded by direct visualization of white zones on the gels, indicating the gelatinolytic activity of proteinases. Gelatinase activity was quantified using the NIH Image program.

Cell Cycle Analysis. A431 cell proliferation was evaluated by measuring DNA content with propidium iodide (PI). In brief, 5 × 10⁴ A431 cells were plated in a 24-well plate in DMEM supplemented with 10% calf serum. In treated wells, MGX was added at three different concentrations (50, 75, and 100 μM). After 3 days of treatment, the cells were treated with trypsin, centrifuged, and fixed with 70% ice-cold ethanol. After 30 min of incubation, the cells were washed in PBS and resuspended in PBS containing 0.02 mg/mL RNase A. After 30 min of additional incubation, 0.01 mg/mL propidium iodide was then added at room temperature for 15 min. The cell cycle was analyzed with a fluorescent analyzer cell sorter (FACS).

Detection of Apoptotic Cell Death. After 72 h of treatment of A431 cells with three different concentrations of MGX (50, 75, and 100 μM), apoptosis was analyzed using the Annexin V-PI kit (R&D Systems GmbH, Wiesbaden, Germany), following the manufacturer's instructions. Briefly both MGX-treated and untreated cells were stained with Annexin-V and PI. Early and late apoptotic cells were determined as Ann V⁺/PI⁻ and Ann V⁺/PI⁺ counts, respectively, as determined by flow cytometry analysis with FACS.

Acknowledgment. We thank T. Chaigneau for excellent technical assistance and Dr. M. Guilloton for his help with the writing of the manuscript.

References and Notes

- 1) Ebringerova, A.; Hromadkova, Z.; Heinze, T. *Adv. Polym. Sci.* **2005**, *186*, 1–67.
- 2) Ebringerova, A.; Heinze, T. *Macromol. Rapid Commun.* **2000**, *21*, 542–556.
- 3) Ebringerova, A.; Hromadkova, Z. *Biotechnol. Genet. Eng. Rev.* **1999**, *16*, 325–346.
- 4) Yamagaki, T.; Tsuji, Y.; Maeda, M.; Nakanishi, H. *Biosci. Biotechnol. Biochem.* **1997**, *61*, 1281–1285.
- 5) Jacobs, A.; Larsson, P. T.; Dahlman, O. *Biomacromolecules* **2001**, *2*, 979–990.
- 6) Teleman, A.; Lundqvist, J.; Tjerneld, F.; Stalbrand, H.; Dahlman, O. *Carbohydr. Res.* **2000**, *329*, 807–815.

- (7) Srivastava, R.; Kulshreshtha, D. *Phytochemistry* **1989**, *28*, 2877–2883.
- (8) Gloaguen, V.; Krausz, P. *SOWF J.* **2004**, *130*, 20–26.
- (9) Paulsen, B. S. *Phytochem. Rev.* **2002**, *1*, 379–387.
- (10) Garbacki, N.; Gloaguen, V.; Bodart, P.; Damas, J.; Angenot, L. *J. Ethnopharmacol.* **1999**, *68*, 235–241.
- (11) Schepetkin, I. A.; Quinn, M. T. *Int. J. Immunopharmacol.* **2006**, *6*, 317–333.
- (12) Paulsen, B. S.; Barsett, H. *Adv. Polym. Sci.* **2005**, *186*, 69–101, and references therein.
- (13) Hashi, M.; Takeshita, T. *Agric. Biol. Chem.* **1997**, *43*, 951–959.
- (14) Hashi, M.; Takeshita, T. *Agric. Biol. Chem.* **1997**, *43*, 961–967.
- (15) Folkman, J. *N. Engl. J. Med.* **1971**, *285*, 1182–1186.
- (16) Alitalo, K.; Tammela, T.; Petrova, T. V. *Nature* **2005**, *438*, 946–953.
- (17) Alèn, R. *Papermaking Sci. Technol.* **2000**, *3*, 11–57.
- (18) Kacurakova, M.; Capek, P.; Sasinkova, V.; Wellner, N.; Ebringerova, A. *Carbohydr. Polym.* **2000**, *43*, 195–203.
- (19) Marchessault, R. H.; Liang, C. Y. *J. Polym. Sci.* **1962**, *59*, 357–378.
- (20) Kacurakova, M.; Wellner, N.; Ebringerova, A.; Hromadkova, Z.; Wilson, R. H.; Belton, P. S. *Food Hydrocoll.* **1999**, *13*, 35–41.
- (21) Gupta, S.; Madan, R. N.; Bansal, M. C. *Tappi J.* **1987**, *70*, 113–114.
- (22) Bartolomé, A. P.; Rupérez, P. *J. Agric. Food Chem.* **1995**, *43*, 608–612.
- (23) Kacurakova, M.; Ebringerova, A.; Hirsch, J.; Hromadkova, Z. *J. Sci. Food Agric.* **1994**, *66*, 423–427.
- (24) Kacurakova, M.; Mathlouthi, M. *Carbohydr. Res.* **1996**, *284*, 145–157.
- (25) Shimizu, K. In *Wood and Cellulosic Chemistry*; Hon, D. N. S., Shiraishi, N., Eds.; Marcel Dekker: New York, 1991; pp 177–214.
- (26) Di Benedetto, M.; Starzec, A.; Vassy, R.; Perret, GY; Crepin, M.; Kraemer, M. *Br. J. Cancer* **2003**, *88*, 1987–1994.
- (27) Guenin, E; Ledoux, D; Oudar, O; Lecouvey, M; Kraemer, M. *Anticancer Res.* **2005**, *25*, 1139–1145.
- (28) Hamma-Kourbali, Y.; Di, Benedetto, M.; Ledoux, D.; Oudar, O.; Leroux, Y.; Lecouvey, M.; Kraemer, M. *Biochem. Biophys. Res. Commun.* **2003**, *310*, 816–823.
- (29) Myoken, Y.; Kayada, Y.; Okamoto, T.; Kan, M.; Sato, G. H.; Sato, J. D. *Proc. Natl. Acad. Sci. U.S.A.* **1991**, *88*, 5819–5823.
- (30) Melnyk, O.; Shuman, M. A.; Kim, K. J. *Cancer Res.* **1996**, *56*, 921–924.
- (31) Malliri, A.; Symons, M.; Hennigan, R. F.; Hurlstone, A. F.; Lamb, R. F.; Wheeler, T.; Ozanne, B. W. *J. Cell Biol.* **1998**, *143*, 1087–1099.
- (32) Heissig, B.; Hattori, K.; Friedrich, M.; Rafii, S.; Werb, Z. *Curr. Opin. Hematol.* **2003**, *10*, 136–141.
- (33) Ebringerova, A.; Kardosova, A.; Hromadkova, Z.; Malovikova, A.; Hribalova, V. *Int. J. Biol. Macromol.* **2002**, *30*, 1–6.
- (34) Kulicke, W. M.; Lettau, A. I.; Thielking, H. *Carbohydr. Res.* **1997**, *297*, 135–143.
- (35) Mazeau, K.; Moine, C.; Krausz, P.; Gloaguen, V. *Carbohydr. Res.* **2005**, *340*, 2752–2760.
- (36) Dubois, M.; Gilles, K. A.; Hamilton, J. K.; Rebers, P. A.; Smith, F. *Anal. Chem.* **1956**, *28*, 350–356.
- (37) Blumenkrantz, N.; Asboe-Hansen, G. *Anal. Biochem.* **1973**, *54*, 484–489.
- (38) Lever, M. *Anal. Biochem.* **1972**, *47*, 273–279.
- (39) Kamerling, J. P.; Gerwig, G. J.; Vliegenhart, J. F. G.; Clamp, J. R. *Biochem. J.* **1975**, *151*, 491–495.
- (40) Montreuil, J.; Bouquet, S.; Debray, H.; Fournet, B.; Spik, G.; Strecker, G. Glycoproteins. In *Carbohydrate Analysis: a Practical Approach*; Chaplin, M. F., Kennedy, J. F., Eds.; IRL Press: Oxford, 1986; pp 143–204.
- (41) Mosmann, T. *J. Immunol. Methods* **1983**, *65*, 55–63.
- (42) Neaud, V.; Faouzi, S.; Guirouilh, J.; Le Bail, B.; Balabaud, C.; Bioulac-Sage, P.; Rosenbaum, J. *Hepatol.* **1997**, *26*, 1458–1466.
- (43) Witczak, Z. J.; Kaplon, P.; Dey, P. M. *Carbohydr. Res.* **2003**, *338*, 11–18.

NP060354P